

Effect of crystal fraction on hardness in FINEMET and NANOPERM nanocomposite alloys

C.-Y. Um^{a)}

Materials Science and Engineering, Carnegie Mellon University, Pittsburgh, Pennsylvania 15213

F. Johnson

National Institute of Standards and Technology, Gaithersburg, Maryland 20899-8552

M. Simone, J. Barrow, and M. E. McHenry

Materials Science and Engineering, Carnegie Mellon University, Pittsburgh, Pennsylvania 15213

(Presented on 8 November 2004; published online 10 May 2005)

Nanocrystallization kinetics of a FINEMET ($\text{Fe}_{71.1}\text{Si}_{18.5}\text{B}_{6.3}\text{Nb}_3\text{Cu}_{1.1}$) and a NANOPERM alloy ($\text{Fe}_{91}\text{Zr}_7\text{B}_2$) were studied and the variation of mechanical properties (hardness) with volume fraction of the crystalline (VFC) phase determined. Time-dependent magnetization and hysteresis loop measurements were used to determine VFC for FINEMET and NANOPERM, respectively. Kinetic results are presented to provide the information necessary to interpret the hardness measurements. Hardness was measured by nanoindentation as a function of VFC to investigate the effect of the evolution of the nanocomposite structure on the mechanical properties. Strengthening mechanisms to understand the linear increase of hardness with the increase of VFC are presented. © 2005 American Institute of Physics. [DOI: 10.1063/1.1855173]

I. INTRODUCTION

FINEMET and NANOPERM alloys are excellent soft magnetic nanocomposite materials with the grain size of their primary crystallization products much smaller than their magnetic exchange length. In attempting to optimize the magnetic properties by controlling the crystallization process, many studies on those magnetic nanocrystalline materials have focused on crystallization kinetics. Only limited attention has been given to the study of hardness (a mechanical property) even though it can play a significant role in influencing the magnetic properties. The stress involved from winding the brittle partially crystallized ribbons on the cores can adversely affect the magnetic properties. Also, this hardness study can produce a useful data for the interpretation of the magnetostriction.

The hardness of large grained materials is well represented by the Hall–Petch relationship (linear hardness increase with grain size decrease). However, as reported frequently in the literature, the Hall–Petch relationship breaks down for grain sizes approaching ~ 10 nm, where the grain size of the alloy systems investigated (FINEMET and NANOPERM) lies. It is therefore plausible that grain-size effects are not the primary determinants influencing the hardness of extremely fine grained materials. We have investigated hardness, by nanoindentation, as a function of the volume fraction of crystalline phase, VFC (as opposed to the grain size) in nanocomposite soft magnets. This paper reports on the results obtained from the hardness measurements as a function of VFC with a proposed model to explain the results.

Crystallization kinetic studies were performed to estimate the VFC using previously published magnetic tech-

niques to compare with those previously reported for similar alloy compositions.^{1–5} The VFC is the important variable for monitoring the crystallization kinetics in the Johnson–Mehl–Avrami (JMA) equation. Here it was measured from isothermal kinetic data (magnetization, M vs time, t) fits to the JMA equation. While the kinetic studies are not new for these alloys, they are important to our interpretation of the evolution of microstructure on hardness.

II. EXPERIMENTAL PROCEDURE

Amorphous ribbon precursors (~ 30 μm in thickness and 3 mm in width) of a NANOPERM alloy with the nominal composition $\text{Fe}_{91}\text{Zr}_7\text{B}_2$ were produced using a single-roller melt spinning technique under an Ar atmosphere. This alloy has lower B concentration by 2 at. % than the base NANOPERM currently being used to investigate the magnetic decoupling of nanograins in alloys where the Curie temperature, T_C^{am} , of the amorphous precursor is lowered to room temperature. Amorphous ribbon precursors of Si-rich FINEMET, 17 μm thick and 35 mm wide, were provided by Spang, Inc. The FINEMET composition was determined to be $\text{Fe}_{71}\text{Si}_9\text{B}_6\text{Nb}_3\text{Cu}_1$ using an inductively coupled plasma (ICP) chemical analysis.

X-ray diffraction (XRD) with Cu $K\alpha$ radiation was used for the verification of amorphous structure of the amorphous ribbon precursors. Differential scanning calorimetry (DSC) measurements were performed at five different heating rates: 5, 10, 20, 40, and 80 °C/min. The magnetic properties as a function of temperature and time were measured with a vibrating-sample magnetometer (VSM) under applied field of 5 kOe. Amorphous ribbon precursors were encapsulated in a quartz tube under vacuum and placed in a furnace to prepare partially crystallized samples with various VFC.

^{a)}Electronic mail: cyum@andrew.cmu.edu

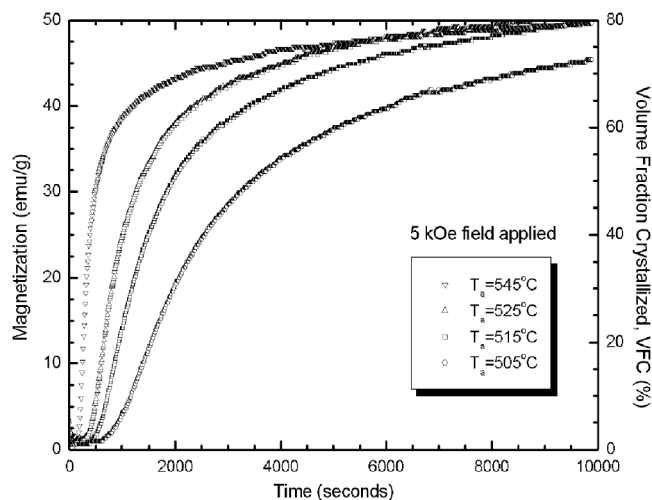


FIG. 1. Magnetization vs annealing time as measured by VSM at temperatures of 505, 515, 525, and 545 °C for the FINEMET alloy with the composition of $\text{Fe}_{71}\text{Si}_9\text{B}_6\text{Nb}_3\text{Cu}_1$. Magnetization is directly proportional to the volume fraction of the crystalline phase (VFC).

Scanning electron microscopy (SEM) was used for the determination of the grain size of coarse-grained iron with 99.97% purity.

The shiny side of ribbon specimens was mechanically polished to a mirror finish with Al_2O_3 powders prior to hardness test using the Nano Indenter XP (MTS Systems Corporation). Continuous stiffness measurement (CSM), with a diamond Berkovich indenter, was used for the indentation experiments. The hardness was calculated based on the stiffness determined from the unloading curve at the final indentation depth of 1000 nm. About 30–40 indents were performed on each specimen to obtain enough statistical significance on the hardness.

III. RESULTS AND DISCUSSION

As well known from the thermomagnetic data, $M(T)$ of FINEMET and NANOPERM alloys, the increase in M at primary crystallization temperature, T_{x1} results from the magnetic phase (bcc α -Fe and DO_3 FeSi, respectively) crystallizing from the nonmagnetic amorphous matrix since T_C^{am} is lower than T_{x1} . The magnetization at T_{x1} is proportional to the VFC, allowing for a JMA kinetic analysis of the isothermal magnetization data at temperatures near T_{x1} .

Figure 1 illustrates the time-dependent magnetization, $M(t)$ near T_{x1} for the FINEMET amorphous precursors. The fits of these isothermal kinetic data to JMA equation yielded an activation energy, Q_{JMA} of 3.6 eV. Analysis of constant heating rate data obtained from DSC measurements and fit to the Kissinger equation yielded an activation energy $Q_{\text{Kissinger}}=3.5$ eV for crystallization. These are comparable to activation energies between 3.4 and 4.5 eV, previously reported for similar FINEMET compositions.^{3–5} A morphology index, n , indicating the dimensionality and mechanism of the crystallization reaction, obtained from the JMA kinetic model was in the range of $n=1.3$ – 1.6 . This is also comparable to those ($n=1.3$ – 2.0) in the reports for the similar FINEMET compositions.^{4,5} The value of the activation energies and n suggests that crystallization occurs quickly in the

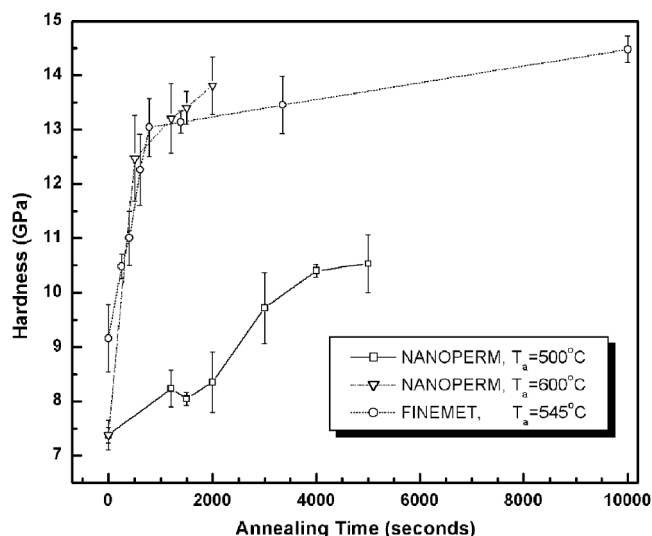


FIG. 2. Hardness vs annealing time for the FINEMET at annealing temperature, $T_a=505$ °C and for the NANOPERM at $T_a=500$ and 600 °C. Error bars on the hardness data indicate the standard deviation calculated from the multiple indentations (30–40) for each sample.

early stages due to the aid of heterogeneous nucleation and more slowly towards the end stages as the early transition-metal diffusion barrier is fully developed.

The VFC for fully crystallized FINEMET has been previously reported by Okumura *et al.*⁶ The VFC of fully crystallized DO_3 FeSi grains (average grain size of ~ 14 – 15 nm) was found to be 75%–80% using transmission electron microscopy (TEM). Therefore, a VFC of 80 was taken to correspond to the 50 emu/g of M of the fully crystallized nanocrystals and then scaled proportionally to the M for partially crystallized nanocomposites. The VFC is shown on the right y axis of the Fig. 1 to be used as a reference. The NANOPERM VFC was estimated by measuring a hysteresis loop at 400 K for the samples previously annealed at 500 and 600 °C for various times. 400 K is well above the T_C^{am} (230 K) and below the Curie temperature of the Fe nanocrystalline grains (993 K). The linear paramagnetic signal from the amorphous matrix was subtracted from the hysteresis loop, leaving the ferromagnetic hysteresis loop of the bcc Fe nanocrystalline grains. Thus, VFC was estimated by comparing the saturation magnetization, M_s obtained from the hysteresis loop to an estimate of the M_s of pure Fe at 400 K (210 emu/g).

Figure 2 shows the hardness data obtained from the nanoindentation experiments of NANOPERM and FINEMET alloys as a function of annealing time for annealing temperatures near T_{x1} . Error bars on the hardness data reflect the standard deviation calculated from the multiple indentations (30–40) for each sample. The hardness is observed to increase with increasing VFC and exhibited similar trends as for the magnetization kinetic data of Fig. 1. JMA analysis applied to the hardness data of NANOPERM yielded $Q_{\text{JMA}} \sim 2.93$ eV, slightly lower than that of base NANOPERM composition ($\text{Fe}_{89}\text{Zr}_7\text{B}_4$) (3–3.4 eV) reported by Hsiao *et al.*¹ This could be due to the lower B concentration by 2 at. % than the base NANOPERM, which reduces the contribution from the diffusion of B atoms to the growth mechanism.

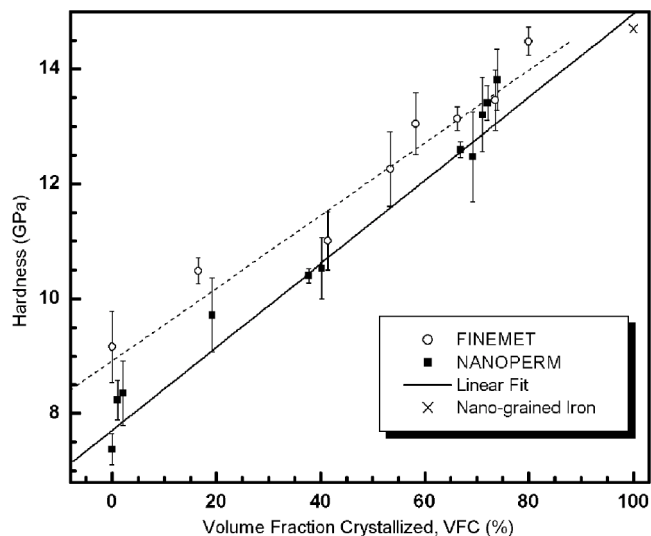


FIG. 3. Hardness vs volume fraction of the crystalline phase (VFC) for the FINEMET and NANOPERM alloys. Error bars on the hardness data indicate the standard deviation. The plot also shows the linear fit to those hardness data points and the hardness of pure Fe with the grain size greater than ~ 13 nm.

Figure 3 shows the hardness variation as a function of VFC for FINEMET and NANOPERM. In both alloys, hardness increased almost linearly with increasing VFC and the fully saturated nanocrystalline alloys exhibited about 1.5 and 2 times higher hardness, respectively, than amorphous precursors. The hardness for $VFC > 74\%$ for NANOPERM and $VFC > 80\%$ for FINEMET was not measured because of the considerable slowing of the growth kinetics as the amorphous region surrounding nanocrystals is enriched in early transition metals at the end of the crystallization process.

In an attempt to compare the hardness of NANOPERM extrapolated to a $VFC=100\%$, with that of nanocrystalline bcc α -Fe (the crystalline phase in NANOPERM), the hardness of coarse-grained bcc α -Fe was measured on the same hardness scale (Berkovich). This hardness value was compared to a Vickers hardness at the same grain size for ball-milled α -Fe polycrystalline materials measured by Malow and Koch.⁷ In their work, the Hall–Petch grain-size dependence of the hardness (increasing hardness linearly with decreasing grain size) was observed for the grain size greater than ~ 13 nm with a plateau region for the grain size smaller, indicating the breakdown of the Hall–Petch relationship. Their Vickers hardness in the plateau region was converted back to the Berkovich hardness scale and shown for comparison in Fig. 3. It is in good agreement with that predicted by the linear extrapolation of the hardness of the NANOPERM to a $VFC=100\%$.

In the work of Malow, no grain-size effect on hardness was observed in the (< 13 nm) nanoscale-grain region (plateau region). This is because the Hall–Petch strengthening mechanism is only viable in the grain-size region where the grain-boundary structure is the same as those of coarse-grained materials. One of the main problems with extrapo-

lating the Hall–Petch behavior to the extremely fine grain sizes is the lack of space for creating the dislocation pileups at a very small grain size. A dispersion or precipitation hardening model, where the particle size is one of the important factors determining hardness, is also not a viable alternative since it is based on the interaction of dislocation with the particles; however, no dislocations exist in the amorphous matrix for NANOPERM and FINEMET alloys. We have pursued a different approach to evaluate the observed hardening in light of solution hardening models where the VFC rather than grain size is the natural variable.

As illustrated in Fig. 3, the clear linear relationship between hardness and VFC indicates that the VFC is the determining factor for the hardness. We propose a model to explain this relationship based on a solid solution hardening mechanism, which is independent of grain size. We postulate that it is the strain introduced into the dense random packing of hard-sphere (DRPHS) atoms in amorphous matrix by virtue of the increasing Zr and B concentrations that accompany their expulsion from the primary nanocrystals. This was corroborated by the independent study of the mechanical properties of amorphous precursors with higher Zr and/or B concentrations.

To investigate the solid solution hardening model further, we produced the amorphous ribbons with a composition of $Fe_{89}Zr_7B_4$ (higher concentration of B by 2 at. %) and $Fe_{85}Zr_9B_6$ (higher concentration of Zr by 2 at. % and B by 4 at. %). The hardness increased from 7.4 GPa (as-cast samples of $Fe_{91}Zr_7B_2$) to 8.5 GPa ($Fe_{89}Zr_7B_4$) and to 9.3 GPa ($Fe_{85}Zr_9B_6$) in these two alloys. As nanocrystallization proceeds, larger Nb (FINEMET) or Zr (NANOPERM) atoms are expelled to the amorphous regions causing what is equivalent to “substitutional solid solution hardening.” It is also plausible that there is a contribution of “interstitial” hardening from the smaller B atoms diffusing into the interstices in the DRPHS amorphous network. Our measurements for the influence of increasing the concentration of glass formers in similar amorphous alloys bear this out.

ACKNOWLEDGMENTS

This work was supported in part by an Air Force Dual Use Science and Technology Contact administered by the Wright Patterson Air Force Base and Magnetics, Inc., a division of Spang, Inc.

¹A. Hsiao, M. E. McHenry, D. E. Laughlin, M. J. Kramer, C. Ashe, and T. Okubo, *IEEE Trans. Magn.* **38**, 2946 (2002).

²M. E. McHenry, M. A. Willard, and D. E. Laughlin, *Prog. Mater. Sci.* **44**, 291 (1999).

³L. K. Varga, E. Bakos, L. F. Kiss, and I. Bakonyi, *Mater. Sci. Eng., A* **179/180**, 567 (1994).

⁴C. F. Conde and A. Conde, *Mater. Lett.* **21**, 409 (1994).

⁵J. Bigot, N. Lecaude, J. C. Perron, C. Milan, C. Ramiarinjaona, and J. F. Rialland, *J. Magn. Mater.* **133**, 299 (1994).

⁶H. Okumura, D. E. Laughlin, and M. E. McHenry, *J. Magn. Mater.* **267**, 347 (2003).

⁷T. R. Malow and C. C. Koch, *Metall. Mater. Trans. A* **29A**, 2285 (1998).